SLAC-TN-10-010

Calculation of Stop Production in Proton-Proton Collisions

Andrea J. Linville
Office of Science, Science Undergraduate Laboratory Internship Program

Washington University, St. Louis, MO

SLAC National Accelerator Laboratory
Menlo Park, CA

August 13, 2009

Prepared in fulfillment of the requirement of the Office of Science, Department of Energy's Science Undergraduate Laboratory Internship under the direction of JoAnne Hewett in the Theoretical Physics division at SLAC National Accelerator Laboratory.

Participant: _____
Signature

Research Advisor: _____
Signature

Work supported in part by US Department of Energy contract DE-AC02-76SF00515.

Table of Contents

I. Abstract ……..……..…….. 3

II. Introduction ……..…..……...…… 4

III. Methods ……..……..... 5

IV. Results ……..……..……..... 10

V. Discussion ……..…….…….……..... 11

VI. Figures …..... 13

VII Acknowledgements ……..……..…… 17

References ……..……..……... 18

I. Abstract

Calculation of Stop Squark Production in Proton-Proton Collisions. ANDREA J. LINVILLE (Washington University, St. Louis, MO 63105) JOANNE HEWETT (SLAC National Accelerator Laboratory, Menlo Park, CA 94025)

Though the Standard Model of particle physics is an elegant theory which has been studied extensively for decades, it leaves many fundamental questions unanswered and is thus widely believed to be incomplete. Possible extensions to the Standard Model (SM) have been postulated and are in the process of being investigated experimentally. The most promising extension is the Minimal Supersymmetric Model (MSSM) which relates every SM particle to a superpartner that differs by ½ unit of spin. The lightest supersymmetric quark, or squark, is expected to be the stop, and the search for this particle is an important experimental task. In this analysis, we use parton-model methods to predict the stop production cross section in proton-proton collisions at LHC energies.

II. Introduction

The Standard Model of particle physics provides a remarkably accurate description of matter at its most elementary level. It explains three of the four known fundamental interactions and the particles that take part in those interactions. Although the Standard Model (SM) is satisfying in its simplicity, it leaves several fundamental questions unanswered and thus it is widely believed that SM is incomplete.

Let us first summarize the SM before discussing extensions to it. In the SM, twelve spin ½ fermions (depicted in Figure 1) are the building blocks of all visible matter. The interactions between these fermions are explained as the result of the exchange of force-mediating bosons, which carry integer spin. The different types of bosons mediate different forces: photons, gluons, and the W and Z bosons respectively carry the electromagnetic force, the strong nuclear force, and the weak nuclear force.

Unfortunately, the SM is inadequate in several respects. First of all, it does not explain why gravity is so weak compared to the other forces. In addition, the Higgs boson, which is predicted by the SM and generates the masses of the fermions and the W and Z bosons, has not yet been observed experimentally. Other shortfalls of the SM are its inability to predict the nature of dark matter and its lack of an explanation for the imbalance between matter and antimatter in the universe. Furthermore, the SM suffers from a number of adjustable parameters, and one would hope that nature could be described without these free parameters.

A widely studied extension of the SM is known as the Minimal Supersymmetric Model (MSSM). Supersymmetry (SUSY) relates each SM elementary particle to a superpartner, or sparticle, which differs from the original particle by a half unit of spin, but otherwise carries identical quantum numbers. Thus, for every fermion in the standard model, there exists a corresponding supersymmetric boson, and vice versa.

SUSY, however, is not a perfect symmetry. If it were exact, each SM particle would be mass-degenerate with its superpartner. Since no superpartners have yet been observed, this implies that if SUSY exists, it must be a broken symmetry in order to allow the sparticles to be relatively heavy. Unfortunately, the masses of the superpartners are highly dependent upon the specific model of SUSY breaking, which is presently unknown.

Any experimental evidence of supersymmetry would have a profound influence on SUSY theory. Towards this end, an extensive search for superpartners is soon to be undertaken at the LHC. Although superpartners have not yet been observed, projections have been made for the production rates of the superpartners of quarks and gluons.

Our objective is to calculate the cross section for the production of the supersymmetric partner of the top quark - the stop - in proton-proton collisions, for stop masses ranging from 200 GeV to 2 TeV.

III. Methods

i. Calculation of $e^+e^- \rightarrow \mu^+\mu$ cross-section

Several preliminary steps were taken before calculating the production rate for the stop squark. These initial computations were performed primarily to check our evaluations of familiar quantities before proceeding to calculate unknown values. First, a program was written (in C++) to calculate the cross-section of the annihilation of a positron and electron to a muon and anti-muon. This SM process involves the s-channel exchange of either a photon or neutral Z boson (see Figure 2), and both contributions were accounted for. The cross-section is yielded by

$$\sigma(e^+e^- \rightarrow \mu^+\mu^-) = Q_\mu^2 Q_e^2 \frac{4\pi\alpha^2}{3s} + \frac{4\alpha}{3}\frac{G_F Q_\mu Q_e}{\sqrt{2}}(g_L + g_R)^2 Re(R) + \frac{4s}{3\pi}\left(\frac{G_F}{\sqrt{2}}\right)^2 (g_L^2 + g_R^2)^2 |R|^2 \quad \textbf{(1)}$$

The first term corresponds to the photon contribution, the second term is a mixed photon-Z boson component, and the third term is a contribution just from the Z boson. Q_μ and Q_e refer to the muon and electron charges, respectively; α is the fine structure constant; $\sqrt{s}$ is the invariant energy of the subprocess; G_F is Fermi's constant; and g_L, g_R, and R are defined as follows:

$$g_L = x_w - ½ \quad \textbf{(2)}$$

$$g_R = x_w \quad \textbf{(3)}$$

and

$$R(s) = \frac{M_Z^2}{s - M_Z^2 + iM_Z\Gamma_Z} \quad \textbf{(4)}$$

In these equations, x_w is the weak mixing angle, M_Z is the mass of the Z boson, and Γ_Z is the decay width of the Z boson. [3]

ii. Modification of equations to calculate $\sigma(q\bar{q} \rightarrow \mu^+\mu^-)$

The original program was then modified to calculate the cross-section of the annihilation of a quark and antiquark to a muon and antimuon, which is known as the Drell-Yan process. This task was accomplished simply by substituting quark charge in place of electron charge and summing over the different types of quarks. Separate cross-section components were set up for the quarks with +2/3 charge (up, charm, and top) and those with -1/3 charge (down, strange, and bottom).

iii. Inclusion of Parton Distribution Functions

In order to generalize the program to obtain the hadronic cross-section $\sigma(pp \rightarrow \mu^+\mu^-)$, the quark cross-sections were combined with parton distribution functions (PDFs). The parton model assumes that a hadron can be described in terms of quasi-free pointlike structures called partons.[3] Therefore, high-energy proton collisions can instead be envisioned as collisions of the quarks, antiquarks, and gluons within the protons. PDFs describe the probability density for

finding a parton with a certain momentum fraction, x, of the momentum, Q^2, that is transferred between the colliding hadrons. The appropriate cross-sections were then multiplied times each parton's PDF and integrated over all momentum fractions:

$$\sigma = \int_0^1 dx_a \int_0^1 dx_b \hat{\sigma} \sum_f [f_A(x_a) f_B(x_b) + f_A(x_b) f_B(x_a)] \quad (5)$$

Here, x_a and x_b are the momentum fractions of parton a and parton b, and the partons originate from proton A or B. The parton-level cross section is represented as $\hat{\sigma}$. The following convenient definition can also be made:

$$\tau \stackrel{def}{=} x_a x_b \quad (6)$$

This is equivalent to

$$\hat{s} = \tau s \quad (7)$$

where $\sqrt{\hat{s}} = Q$ is called the scattering energy or the invariant mass, and $\sqrt{s}$ is known as the proton center-of-mass energy or "machine" energy. Equation 5 can subsequently be written as

$$\sigma = \int_0^1 d\tau \int_\tau^1 dx_a \hat{\sigma} \sum_f [f_A(x_a) f_B(\tau/x_a) + f_A(\tau/x_a) f_B(x_a)] \quad (8)$$

Calculations were performed by utilizing the PDF set CTEQ6, from the Coordinated Theoretical-Experimental QCD collaboration, and all integrals were evaluated with the VEGAS integration routine.[6] VEGAS is a form of Monte Carlo integration which estimates the value of a multidimensional definite integral by evaluating the integrand at randomly chosen points.

These calculations enabled us to plot the total muon production cross-section as a function of Q (the invariant muon mass). The proton center-of-mass energy was taken to be 14 TeV, which is the projected eventual energy of the LHC, and the integrals were evaluated for Q between 50 GeV to 2 TeV, in 1 GeV increments.

iv. Setup of $\sigma(pp \rightarrow \tilde{q}\bar{\tilde{q}})$ calculation

The next step was to replace the quark to muon cross-sections with those for the various channels which produce a squark and an antisquark. Three different initial states can result in squark pair production from proton-proton collision: $qq \rightarrow \tilde{q}\tilde{q}$, $q\bar{q} \rightarrow \tilde{q}\bar{\tilde{q}}$, and $gg \rightarrow \tilde{q}\bar{\tilde{q}}$. Before calculating the cross-section for each case, it is convenient to define the quantities [3]

$$\mathscr{S} = [s-(m_1+m_2)^2]^{1/2}[s-(m_1-m_2)^2]^{1/2}\,, \tag{9}$$

$$\Delta_{ai} = M_a{}^2 - m_i{}^2\,, \tag{10}$$

and

$$\Lambda_a = \ln\left[\frac{s+\Delta_{a1}+\Delta_{a2}-\mathscr{S}}{s+\Delta_{a1}+\Delta_{a2}+\mathscr{S}}\right] \tag{11}$$

where m_1 and m_2 are the masses of the produced squarks, and M_a refers to the mass of the particle exchanged in either the t- or u-channel, depending upon which Feynman diagram we are examining. With these definitions, the cross-sections for the aforementioned annihilations are:

$$\sigma(q_iq_j\rightarrow\tilde{q}_i\tilde{q}_j) = \frac{4\pi\alpha_s{}^2}{9s^2}\left[\left[-2\mathscr{S}-(s+\Delta_{ti}+\Delta_{tj})\Lambda_t+\frac{1}{1+\delta_{ij}}\frac{\mathscr{S}sm_{\tilde{g}}{}^2}{\Delta_{ti}\Delta_{tj}+sm_{\tilde{g}}{}^2}+\tfrac{1}{3}\delta_{ij}\frac{sm_{\tilde{g}}{}^2}{s+\Delta_{ti}+\Delta_{tj}}\Lambda_t\right]+\delta_{ij}(t\rightarrow u)\right], \tag{12}$$

$$\sigma(q_i\bar{q}_j\rightarrow\tilde{q}_i\tilde{q}^*_j) = \frac{4\pi\alpha_s{}^2}{27s^2}\left[\delta_{ij}\left[\frac{\mathscr{S}^3}{s^2}+\frac{\mathscr{S}(s+\Delta_{ti}+\Delta_{tj})}{s}+\frac{2(\Delta_{ti}\Delta_{tj}+m_{\tilde{g}}{}^2s)}{s}\Lambda_t\right]+3\left[-2\mathscr{S}-(s+\Delta_{ti}+\Delta_{tj})\Lambda_t+\frac{\mathscr{S}sm_{\tilde{g}}{}^2}{sm_{\tilde{g}}{}^2+\Delta_{ti}\Delta_{tj}}\right]\right], \tag{13}$$

and

$$\sigma(gg\rightarrow\tilde{q}_i\tilde{q}^*_i) = \frac{\pi\alpha_s{}^2}{3s^2}\left[\left[\frac{5}{8}+\frac{31}{4}\frac{m^2}{s}\right]\mathscr{S}+\left[4+\frac{m^2}{s}\right]m^2\ln\left[\frac{s-\mathscr{S}}{s+\mathscr{S}}\right]\right] \tag{14}$$

v. Calculation of $\sigma(pp \rightarrow \tilde{t}\bar{\tilde{t}})$

Fortunately, equations 12-14 simplify considerably since we are presently only interested in processes resulting in a stop and anti-stop, rather than any squark pair. If one were to look at the production of any squark and antisquark, all the processes shown in the Feynman diagrams in Figure 3 would be possible. However, the Feynman rules that require conservation of charge and conservation of quark flavor at each vertex reduce the number of channels available for the production of a stop and anti-stop. For example, in the quark-antiquark t-channel, flavor conservation requires that the initial quark and antiquark must be a top and anti-top. Since top quarks carry such a tiny fraction of a proton's momentum, this particular channel has essentially no probability of actually occurring. For the same reasons, both the t- and u- channels of quark-quark annihilation are not present in the top quark scenario. So, one need only calculate cross-sections for the processes shown in Figure 4.

Thus, equation 12 is not required here (and hence equations 10 or 11 are not needed either!), and equation 13 reduces to

$$\sigma(q_i\bar{q}_i \rightarrow \tilde{q}_j\tilde{q}_j^*) = \frac{4\pi{\alpha_s}^2}{27s^4}\mathscr{S}^3 \qquad \textbf{(15)}$$

Equation 8 is then utilized again, with the incorporation of the applicable parton cross-sections and the corresponding PDFs, and the modification of the lower integration limit to ensure that enough energy is present to produce the stop quark pair. Finally, the total cross-section for stop production following proton-proton collision can be calculated.

IV. Results

i. Calculation of $\sigma(e^+e^- \rightarrow \mu^+\mu)$

The cross-section for $e^+e^- \rightarrow \gamma, Z \rightarrow \mu^+\mu^-$ was calculated to be 61.6 fb.

ii. Parton Distributions

Parton densities for the u, d, c, and s quarks and anti-quarks are graphed in Figures 5-7 for Q = $\sqrt{2}, \sqrt{20}$, and $\sqrt{200}$ GeV, respectively. The densities for b and t quarks were negligible at these scattering energies and are therefore omitted from the plots.

iii. Calculation of $\sigma(pp \rightarrow \mu^+\mu^-)$

Figure 8 shows the $pp \rightarrow \mu^+\mu^-$ cross-section for invariant muon masses from 50 GeV to 2 TeV. A peak in the cross-section was observed at 91 GeV±0.5, where it has a maximum value of 0.88 nb. When M = 500 GeV, the cross-section has a value of 0.96 fb. At the upper mass limit, the cross-section trails off to 0.731 ab at 2 TeV.

iv. Calculation of $\sigma(pp \rightarrow \tilde{t}\bar{\tilde{t}})$

In Figure 9, the $pp \rightarrow \tilde{t}\bar{\tilde{t}}$ cross-section is shown for stop masses between 200 GeV and 2 TeV. The maximum cross-section occurs at 200 GeV, with a value of 271 pb and a standard deviation of 1.03 pb. This standard deviation results from the accuracy of the VEGAS integration routine, which could be increased by setting the program to calculate the value of the integrand at a greater number of points.[1] The cross-section decreases steadily to 227 ab (±0.431 ab) at 2 TeV.

[1] The primary drawback to evaluating the integrals at more points is the increased CPU usage that is required.

V. Discussion

i. Calculation of $\sigma(e^+e^- \rightarrow \mu^+\mu^-)$

The electron-positron annihilation cross section is well known, and our value agrees well with previous data. [7]

ii. Parton Distributions

The parton distribution results also closely match previous work,[2] though the correspondence is not exact. Discrepancies most likely result from utilizing different parameterizations of the parton densities. Modifications to PDFs have been made frequently, with different estimates of strong-interaction corrections to elementary parton distributions. While the most recent parameterization, CTEQ6, was applied in this study, many other versions have been used previously. The uncertainty due to these differences is less than 10% at the LHC [4]. Nevertheless, the general trends of the distributions match expectations. At lower scattering energies, the up and down quarks tend to have the greatest probability of interacting. This is logical since the up and down quarks are the only so-called "valence" quarks within the proton. Valence quarks are the only ones that contribute to a hadron's quantum numbers. The other quarks and the antiquarks are still present in protons as highly unstable "sea" quarks, virtual quark-antiquark pairs formed from the splitting of gluons within the proton. At low scattering energies, sea quarks are confined within hadrons and have minimal contributions to the overall cross-sections. Much more scattering energy is required to enable the sea quarks to collide with partons from the other proton. As can be seen in Figures 5-7, the sea quarks play a more substantial role at higher scattering energies, though the bottom and top quark contributions remain negligible for all the energies plotted.

[2] Conducted by Michael Peskin, SLAC

iii. Calculation of $\sigma(pp \rightarrow \mu^+\mu^-)$

The muon production cross-section also demonstrates the expected trend. The resonance in the cross-section at a dimuon mass of 91 GeV corresponds to the mass of the Z boson. An invariant mass of 91 GeV enables the production of a Z boson, which subsequently decays into two highly energetic muons.

Literature states that the expected differential cross-section at a dimuon mass of 500 GeV is ~1 fb,[5] quite close to the calculated value of 0.96 fb. Some error results from the utilization of different parton distributions in these calculations. Additionally, taking data at finer increments would have obviously yielded increased accuracy.

iv. Calculation of $\sigma(pp \rightarrow \tilde{t}\bar{\tilde{t}})$

Finally, the stop cross-section agrees well, though not perfectly, with that determined by Dawson, et.al.[3]. The values differ because we examine only the leading order (LO) Feynman diagrams, while others have incorporated next-to-leading order (NLO). If NLO corrections were to be included, the cross-sections would be increased to values above the LO predictions.

The stop production cross section depends essentially only on the masses of the produced stops. So, after experimentally establishing bounds on the stop production cross-section, the cross-section can be used to ascertain a lower bound on the stop mass. Similarly, if stops are observed, the cross-section can subsequently be employed to determine the masses of the stop particles, which would be of use in pinpointing the specific model of SUSY breaking.[4]

Thus, our projections of the production rates of stop squarks in high-energy collisions are of value both in interpreting data and in preparing new experimental searches for supersymmetry.

VI. Figures

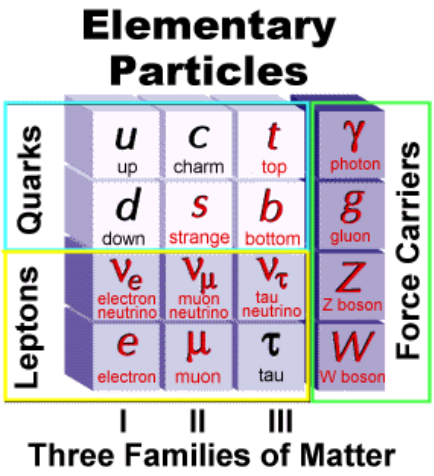

Figure 1 - Summary of Standard Model Elementary Particles [1]

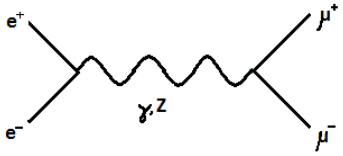

Figure 2 - Feynman diagram of electron-positron annihilation

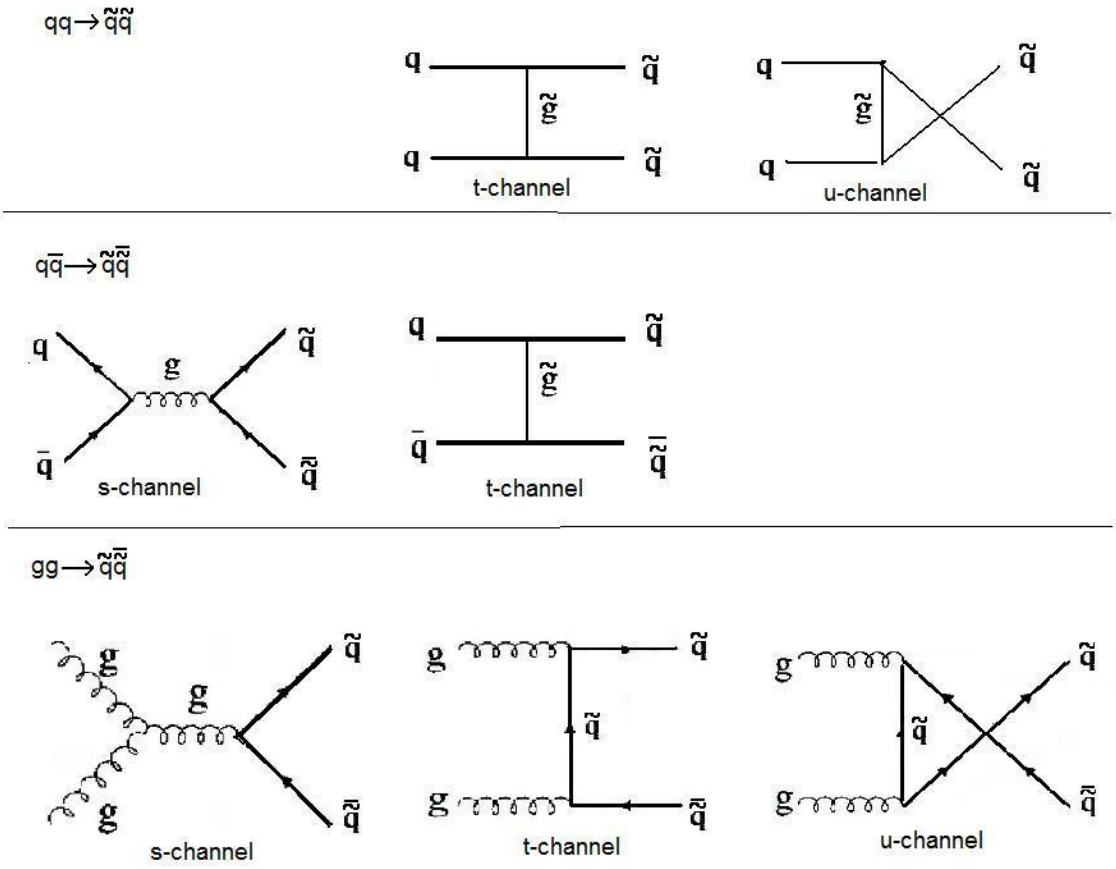

Figure 3 - Feynman diagrams for all processes producing a squark and anti-squark [4]

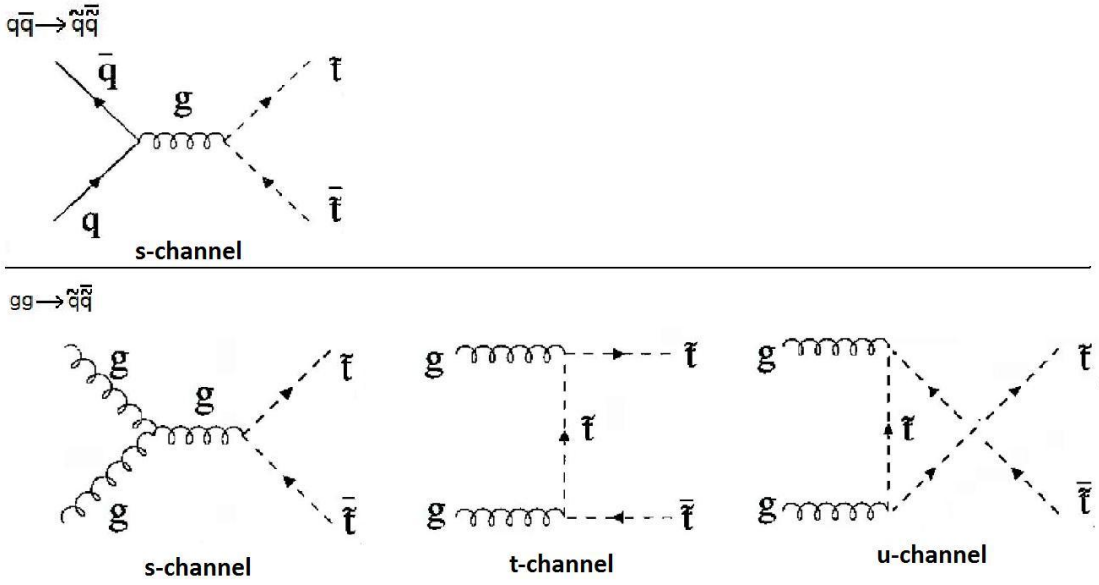

Figure 4 - Feynman diagrams for production of a stop and anti-stop

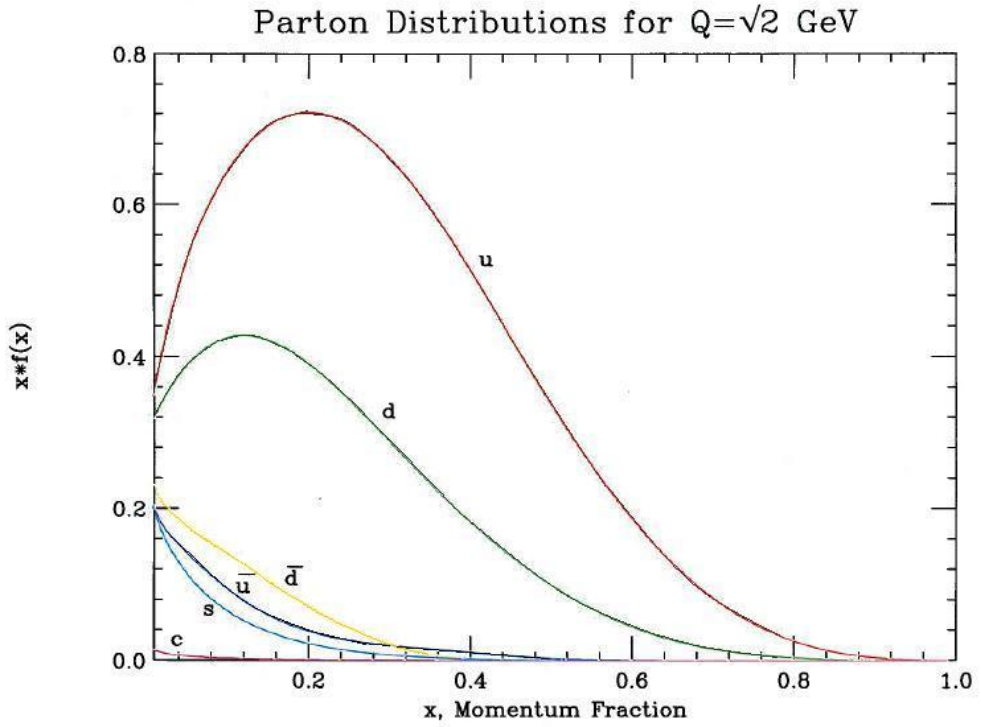

Figure 5 - Parton densities calculated using CTEQ6 PDFs, with scattering energy Q = √2 GeV

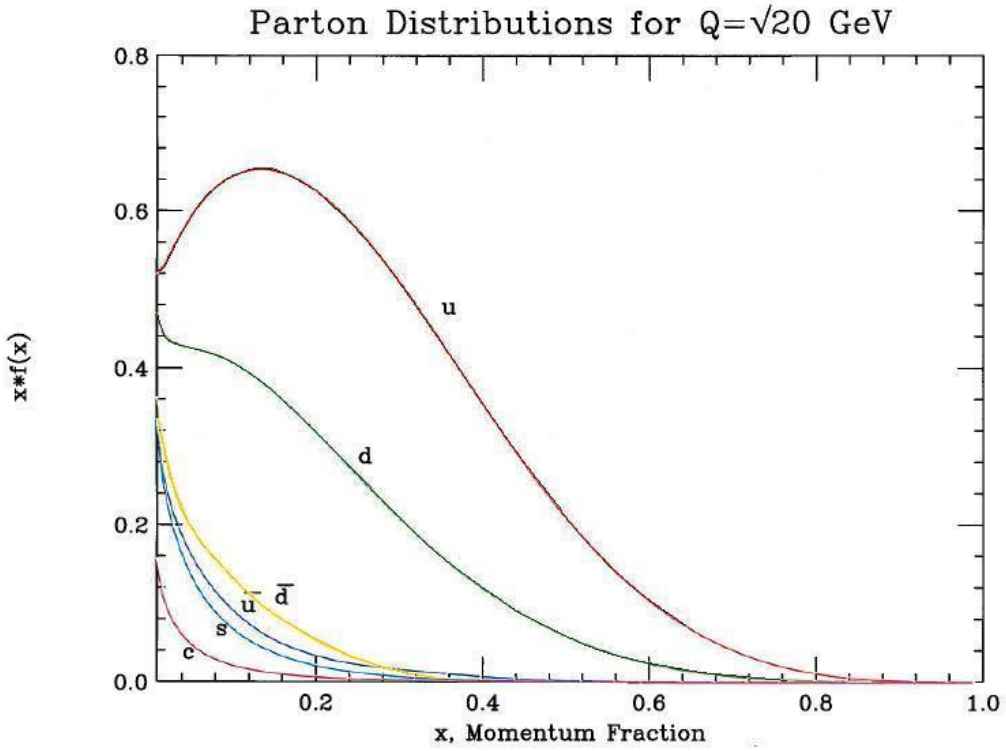

Figure 6 - Parton densities for Q = √20 GeV

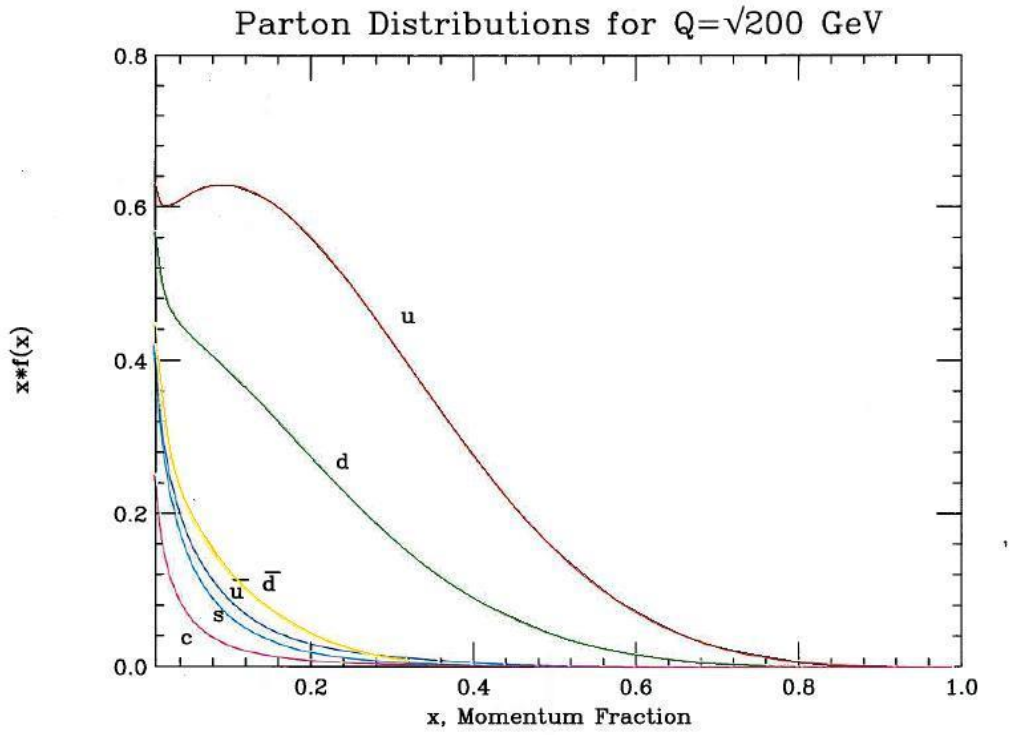

Figure 7 - Parton densities for Q = √200 GeV

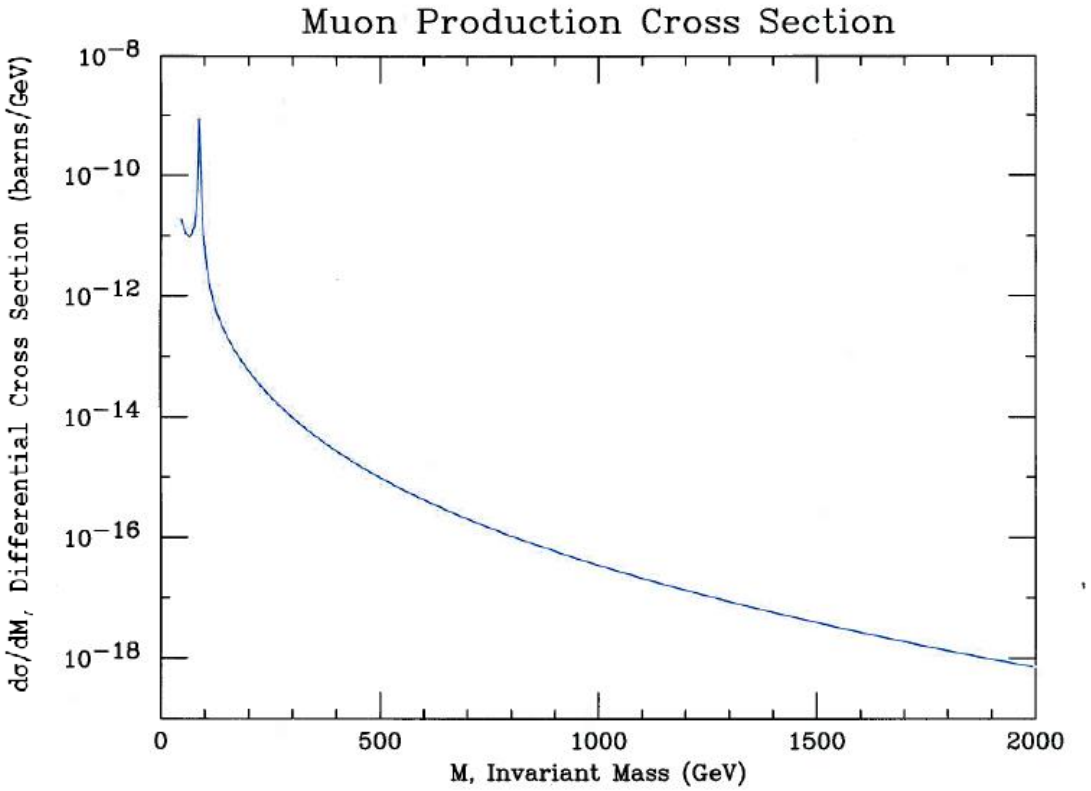

Figure 8 – Differential cross-section for p-p annihilation to muons, at center of mass energy = 14 TeV

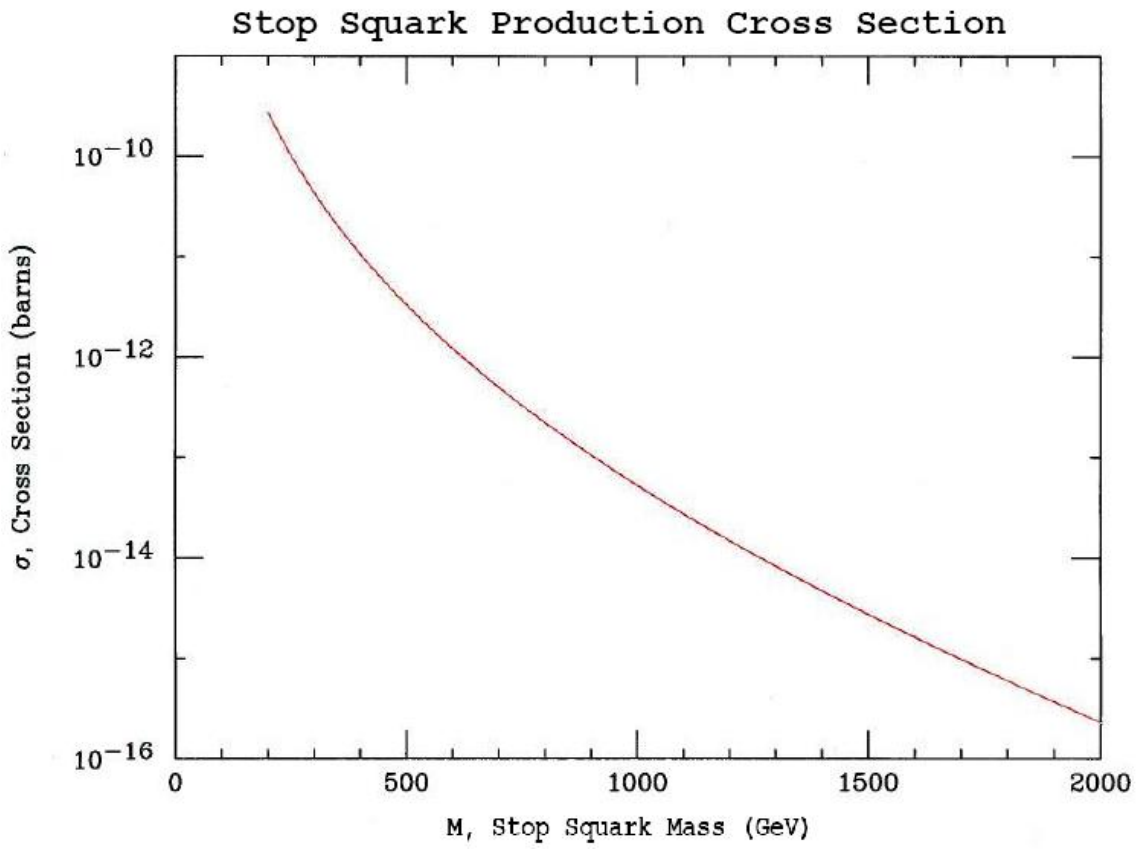

Figure 9 - Cross-section for p-p annihilation to stop-antistop, at center of mass energy = 14TeV

VII. Acknowledgements

I would like to thank my mentors, JoAnne Hewett and Tom Rizzo, for all their time and assistance. Also, many thanks to Michael Peskin for providing me with the VEGAS integration programs. Lastly, I would like to sincerely thank John Conley, Randel Cotta, and James Gainer for their programming help and their patience with all my questions.

References

[1] C.M.S. Collaboration, "The CMS Physics Technical Design Report, Volume 2," CERN/LHCC, vol. 2006/021, no. CMS TDR 8.2.

[2] M. Woods. "Standard Model of Particle Physics." http://www-sldnt.slac.stanford.edu/alr/standard_model.htm, April 9, 2001 [July 17, 2009]

[3] S. Dawson, E. Eichten, and C. Quigg. "Search for supersymmetric particles in hadron-hadron collisions," *Physical Review D*, vol. 31, no. 7, pp. 1581-1637, 1 April 1985.

[4] W. Beenakker, M. Krämer, T. Plehn, M. Spira, and P.M. Zerwas. "Stop Production at Hadron Colliders," *Nuclear Physics B*, vol. 515, pp. 3-14, 1998.

[5] M. Schott. "Z Boson Production at LHC with First Data," *The 2007 Europhysics Conference on High Energy Physics Journal of Physics*, Conference Series 110, 2008.

[6] P. Nadolsky "CTEQ6 Parton Distributions." http://hep.pa.msu.edu/cteq/public/cteq6.html Jan 28, 2009 [July 2009]

[7] Elsevier publishing, *Physics Letters B*, vol. 667, Issues 1-5, 18 September 2008.